Journal of Statistical Physics, Vol. 66, Nos. 3/4, 1992

Universality Class of Interface Growth with Reflection Symmetry

P. Devillard[1] **and H. Spohn**[1]

Received May 23, 1991

We investigate interface dynamics in $1+1$ dimensions, respecting reflection symmetry. In the continuum approach of Kardar, Parisi, and Zhang, the leading nonlinearity is then of the form $(\nabla h_t)^3$. On the basis of Monte Carlo simulations for a driven lattice gas, we argue that the nonlinearity is marginally irrelevant. Thus, the universality class is the one of equilibrium interfaces with a purely relaxational bulk dynamics.

KEY WORDS: Interface growth; driven lattice gas; fluctuation phenomena; random processes.

1. INTRODUCTION

Recently, Derrida *et al.*[1] studied the fluctuations of an interface in a two-dimensional cellular automaton (the Toom model) at low noise strength. The particular dynamical rules are of no importance here. The reader should only know that for the orientation chosen, the interface dynamics is symmetric under reflection relative to the average location. Such a symmetry is well known for equilibrium interfaces. It came as a surprise to find this feature also in nonequilibrium. In ref. 1 it was argued, following the approach of Kardar *et al.*,[2] that on a sufficiently coarse scale the one-dimensional interface is governed by

$$\frac{\partial h_t}{\partial t} = -v\frac{\partial h_t}{\partial x} - \lambda\left(\frac{\partial h_t}{\partial x}\right)^3 + \nu\frac{\partial^2 h_t}{\partial x^2} + \eta_t \tag{1}$$

[1] Theoretische Physik, Ludwig-Maximilians-Universität München, Theresienstrasse 37, D-8000 Munich 2, Germany.

0022-4715/92/0200-1089$06.50/0

Here, $h_t(x)$ is the height of the interface above the point x of a reference line. The term $\nu\,\partial^2 h_t/\partial x^2$ describes the smoothening due to rigidity against bending. η_t is white noise with covariance

$$\langle \eta_t(x)\,\eta_{t'}(x')\rangle = \gamma\delta(t-t')\,\delta(x-x') \tag{2}$$

The first two terms come from a gradient expansion of the orientation-dependent interface velocity. In order to respect the symmetry $h_t \to -h_t$, the even terms in this expansion must vanish.

In ref. 1, only the linear theory ($\lambda = 0$) was studied theoretically, leaving open whether the large-scale properties of the interface would be modified by the cubic nonlinearity $\lambda(\partial h_t/\partial x)^3$. The numerical simulation of the Toom model was inconclusive in that respect. Some features, such as interface correlations, are in accordance with the linear theory. On the other hand, the width of an initially flat interface was found to grow faster than predicted by linear theory. In this contribution, our goal is to understand whether Eq. (1) defines a new universality class of surface growth. Since $\lambda(\partial h_t/\partial x)^3$ scales as $\nu(\partial^2 h_t/\partial x^2)$ and the noise, the problem is whether the cubic nonlinearity is marginally relevant or not. This will be investigated in the context of $(1+1)$-dimensional models.

2. DRIVEN LATTICE GAS

Since the issue is universality, *a priori* we have a wide choice of growth models. In particular, there is no reason to stick to the effective interface model derived from the Toom dynamics in the low-noise approximation. From our experience with growth models we know that scaling regimes may differ widely.[3,4] Thus, our freedom must be used so to minimize crossover effects. We only require:

(i) $h_t \to -h_t$ symmetry

(ii) A continuously tunable λ

(iii) Theoretical and numerical simplicity

For one-dimensional interfaces, it is more convenient to consider the interface slope. It is governed by a stochastic exchange dynamics with conservation law. Physically, the slope dynamics can be viewed also as a driven lattice gas or as a Ginzburg–Landau type B model. Only for an equilibrium interface does the lattice gas satisfy detailed balance. We have tried several models, including variations on the Toom interface dynamics and a discretization of Eq. (1). The by far most convincing results are obtained from a simple nearest neighbor exchange dynamics. To define it, we need a little bit of notation.

We consider spins $\sigma_j = \pm 1$ on a one-dimensional lattice, $j = 1,..., L$, with periodic boundary conditions ($\sigma_{L+1} = \sigma_1$). A whole spin configuration is denoted by σ. The dynamics is given through nearest neighbor spin exchanges. The rate to exchange the spins σ_j and σ_{j+1} is $c_{j,j+1}(\sigma)$, which is assumed to depend only on the two nearest neighbors, σ_{j-1} and σ_{j+2}, of the bond $(j, j+1)$. If we require reflection symmetry $\sigma \to -\sigma$, then the most general form of the exchange rates is as shown in Fig. 1 with $\alpha_1, \alpha_2, \alpha_3, \alpha_4 \geqslant 0$. In terms of the spin variables, we have

$$\begin{aligned} c_{j,j+1}(\sigma) = {} & \tfrac{1}{16}(1+\sigma_j)(1-\sigma_{j+1})[(\alpha_1+\alpha_2+\alpha_3+\alpha_4) \\ & + (\alpha_1+\alpha_2-\alpha_3-\alpha_4)\sigma_{j-1} \\ & + (\alpha_1-\alpha_2+\alpha_3-\alpha_4)\sigma_{j+2} + (\alpha_1-\alpha_2-\alpha_3+\alpha_4)\sigma_{j-1}\sigma_{j+2}] \\ & + \tfrac{1}{16}(1-\sigma_j)(1+\sigma_{j+1})[(\alpha_1+\alpha_2+\alpha_3+\alpha_4) \\ & + (-\alpha_1-\alpha_2+\alpha_3+\alpha_4)\sigma_{j-1} \\ & + (-\alpha_1+\alpha_2-\alpha_3+\alpha_4)\sigma_{j+2} \\ & + (\alpha_1-\alpha_2-\alpha_3+\alpha_4)\sigma_{j-1}\sigma_{j+2}] \end{aligned} \tag{3}$$

The probability distribution on spin configurations is governed by the master equation

$$\frac{d}{dt}\rho_t(\sigma) = \sum_{j=1}^{L} c_{j,j+1}(\sigma^{j,j+1})\rho_t(\sigma^{j,j+1}) - c_{j,j+1}(\sigma)\,\rho_t(\sigma) \tag{4}$$

where $\sigma^{i,j}$ denotes the spin configuration σ with the spins at sites i and j exchanged. To avoid wiggles on the scale of the lattice constant, we define height differences as

$$h_t(x+1) - h_t(x) = [\sigma_{x+1}(t) + \sigma_x(t)]/2 \tag{5}$$

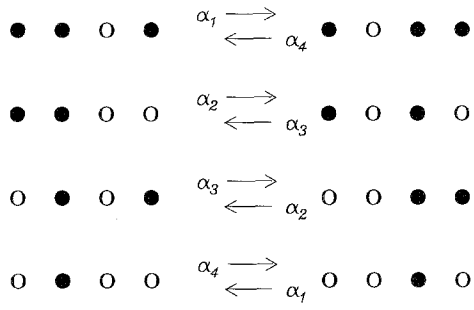

Fig. 1. Rates for the nearest neighbor spin exchange dynamics.

with $\sigma(t)$ the spin configuration at time t. From (5), we obtain the height $h_t(x)$ by integration starting with $h_t(1)$. We only have to take into account that this references point is changing itself in time and is given by the spin current through the bond $(N, 1)$ integrated up to time t. Clearly, the average slope

$$m = \frac{1}{L} \sum_{j=1}^{L} \sigma_j(t) \tag{6}$$

is conserved. Modulo that slope, $h_t(x)$ is periodic with period L.

In passing, we mention that the slope of the Toom interface is also governed by a spin exchange dynamics: in the case of a symmetric noise, a spin searches for the first spin with opposite sign to the right and the pair is exchanged with rate one. Thus, the exchange rates are of arbitrary range. Modifications are, e.g., to restrict the search rule to a maximal range.

If we define an "inverse temperature" β through

$$\frac{\alpha_2}{\alpha_3} = e^{4\beta} \tag{7}$$

then for

$$\alpha_1 = \alpha_4 \tag{8}$$

the exchange rates (3) are those of a spin chain with Kawasaki dynamics. For fixed magnetization m, the steady state $\rho^{(S)}(\sigma)$ for the master equation (4) is given by

$$\rho^{(S)}(\sigma) = \frac{1}{Z} \exp\left(\beta \sum_{j=1}^{L} \sigma_j \sigma_{j+1}\right) \tag{9}$$

which we recognize as the one-dimensional nearest neighbor Ising model. The exchange rates satisfy detailed balance with respect to $\rho^{(S)}(\sigma)$. Large-scale fluctuations in the magnetization are governed by fluctuating hydrodynamics. These are equations of the form (1), (2) with $v = 0 = \lambda$, ν the bulk diffusion coefficient, and $\gamma = \chi/2\nu$, with χ the static compressibility.

To our surprise, even if $\alpha_1 \neq \alpha_4$, the stationary solution to the master equation (4) with fixed m is still given by (9). However, detailed balance is now violated. One way to convince oneself is by computing the average current $j(m)$ as a function of the magnetization. In the limit $L \to \infty$, we obtain

$$j(m) = \tfrac{1}{2}(\alpha_4 - \alpha_1)(-m + \langle \sigma_0 \sigma_1 \sigma_2 \rangle_m) \tag{10}$$

where $\langle \cdot \rangle_m$ denotes the expectation with respect to (9) for fixed m in the limit $L \to \infty$. The three-point correlation is computable through the transfer matrix, but the resulting expression is not very illuminating. Therefore we only note that $j(m) = -j(-m)$ and $j(-1) = j(0) = j(1) = 0$. $j(m)$ has the shape of a cubic polynomial with a single maximum and minimum inside $[-1, 1]$.

We return to the interface dynamics. Reflection symmetry requires that we choose L even and an equal number of up and down spins, i.e., $m = 0$. To make contact with the continuum theory (1), (2), we would like to identify the coefficients there in terms of the spin model. For this purpose we observe that an interface with slope m progresses along the h axis with velocity $j(m)$. Thus, we set ($' = d/dm$)

$$v = j'(0) = -\tfrac{1}{2}(\alpha_4 - \alpha_1)(1 - \tanh \beta)^2 \tag{11}$$

$$\lambda = \tfrac{1}{6} j'''(0) = \tfrac{1}{2}(\alpha_4 - \alpha_1)(1 - \tanh \beta)^3 (1 + \tanh \beta)^{-1} \tag{12}$$

Equations (11), (12) should not be taken literally, because we compare fully renormalized coefficients from $j(m)$ with bare coefficients in (1). At the present stage, v and γ cannot be obtained separately, only their ratio

$$\frac{\gamma}{2v} = \chi = (1 + \tanh \beta)(1 - \tanh \beta)^{-1} \tag{13}$$

which follows by equating the spatial interface fluctuations in the steady state for (1), (2) and for (4). Equation (12) shows that $\lambda \to 0$ for $\beta \to \infty$ (ferromagnetic steady state) and that $\lambda \to \infty$ for $\beta \to -\infty$ (antiferromagnetic steady state). More importantly, if we fix $\alpha_4 - \alpha_1$ and consider a range of β such that the correlation length is less than three lattice constants, then λ varies over three decades. Therefore, we can reach strong nonlinearities without one of the rates becoming too small.

3. MONTE CARLO SIMULATIONS

We simulated the nearest neighbor exchange dynamics defined by the rates of Eq. (3) and with periodic boundary conditions. Since we are interested in systems where detailed balance is violated, we chose $\alpha_1 \neq \alpha_4$ and varied the nonlinear coupling constant λ through the ratio α_2/α_3. The continuous-time master equation (4) corresponds to sequential random updating. For reasons of speed, we prefer parallel updating implemented as follows. The lattice is partitioned into four sublattices. Two neighboring sublattices are chosen at random. Then, in parallel, each pair of neighboring spins is exchanged with probability α_1, α_2, α_3, α_4 according to

Fig. 1. We avoid the formation of fronts by choosing $\alpha_1 = \alpha_2 = 1/2$ (rather than $\alpha_1 = \alpha_2 = 1$). Simulations were carried out with a fully vectorized multispin coding algorithm[5] which was run on Cray YMPs. We checked that an independently written nonmultispin program gave results consistent with those of the multispin program.

In general, the large-scale behavior of interfaces is characterized by two scaling exponents, the static exponent ζ (which governs the typical spatial fluctuations of a dynamically stationary piece of the interface) and the dynamic exponent z (which governs the temporal spreading of interface fluctuations). In our model, the steady state for the interface slope has a finite correction length. Therefore, the static exponent is given by

$$\zeta = 1/2 \tag{14}$$

To determine the dynamic exponent, we follow the standard route and consider the width $w(t)$ of the interface defined as

$$w(t)^2 = \langle (h_t - \langle h_t \rangle)^2 \rangle \tag{15}$$

where the brackets refer to the spatial average over all sites $j = 1,..., L$. Initially, $h_0(x) = 0$, which corresponds to a configuration of alternating + and − spins. The width should scale as

$$w(t) \sim t^{\zeta/z} \tag{16}$$

for $1 \ll t \ll L^z$. Time t is measured in unit of Monte Carlo attempts per spin. Figure 2 shows $w(t)^2$ versus t for different values of the ratio α_2/α_3 [compare with Eq. (7)]. As explained before, we chose $\alpha_1 = \alpha_2 = 1/2$. The

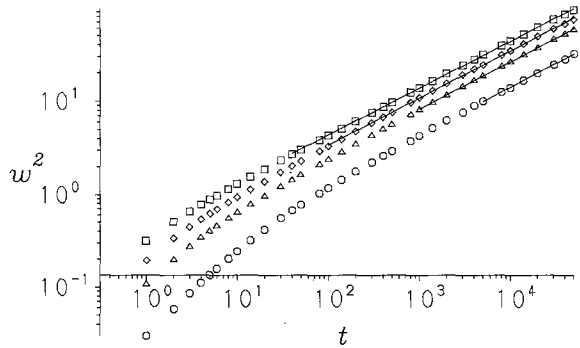

Fig. 2. Log-log plot of the squared width w^2 versus time t for the driven lattice gas with parameters $\alpha_1 = \alpha_2 = \frac{1}{2}$. Curves are, respectively, from top to bottom, for $\alpha_3 = \alpha_4 = \frac{1}{4}$ (□), $\frac{1}{8}$ (◇), and $\frac{1}{64}$ (○). The system sizes are $L = 5120$. Averages have been taken over 512 samples. The symbols are much larger than the typical spread of the points around the fit straight lines.

coupling constant is increased by setting $\alpha_3 = \alpha_4 = 1/2^n$ with $n = 2, 3, 4, 6$. The system sizes are $L = 5120$ and averages have been taken over 512 samples up to $t = 5 \times 10^4$.

We analyze the data by first determining effective exponents in successive time intervals $[t_n, t_{n+1}]$. Beyond a certain time, which increases with the coupling constant, the effective exponent becomes independent of the interval (within the error bars). To obtain then the optimal value for z, we make a least square fit in an interval $[t_-, t_+]$, where t_- is in a region where the effective exponent has reached a constant value and $t_+ = 5 \times 10^4$. The number of data points used is much larger than the number of symbols drawn in Fig. 1. Numerical values for the dynamic exponent z can be found in Table I. For example, for $\alpha_2/\alpha_3 = 2$, a least square fit in the interval $40 < t < 5 \times 10^4$ gives $z = 2.009 \pm 0.015$. Simulations of systems of smaller sizes together with finite-size scaling did not suggest $z \neq 2$ in the asymptotic limit $L \to \infty$.

For short times, typically $t < 1 \ldots 100$, depending on the ratio α_2/α_3, $w(t)$ increases faster than $t^{1/4}$. This initial regime can be explained qualitatively in the following fashion. Since $\alpha_3/\alpha_2 \ll 1$, at first, a dilute gas of elementary terraces of height ± 1 and width 1 is formed. Because $\alpha_1 \neq \alpha_4$, these terraces drift to the right and can either grow in a diffusive fashion or be annihilated as the two ledges of the terrace meet. Initially, the density of terraces is proportional to t, implying $w(t) \sim t^{1/2}$. The crossover sets in when steps collide.

The scaling of the interface reappears in the dynamical structure function $S(x, t)$ in real space defined as

$$S(x, t) = \langle \sigma_{x_0}(t_0) \sigma_{x+x_0}(t+t_0) \rangle \tag{17}$$

where the brackets refer to the average over the stationary measure. By translational invariance, it is independent of x_0 and t_0, but in practice, to obtain good statistics, we average over all x_0 from 1 to L and over different

Table I. Numerical Values for the Exponent z for Different Values of α_2/α_3 [a]

α_2/α_3	t_-	t_+	z	Δz
2	40	5×10^4	2.009	0.015
4	100	5×10^4	2.00	0.03
8	1000	5×10^4	1.995	0.04
32	5000	5×10^4	1.97	0.08

[a] Our values of z are obtained from least square fits of the curve $\log w^2(t)$ versus $\log t$ in intervals $[t_-, t_+]$. We keep $\alpha_1 = \alpha_2 = 1/2$ and $\alpha_3 = \alpha_4$. Here Δz is the uncertainty in z.

values of t_0 (typically ten values). In order to establish a stationary state, we start from a random spin configuration and let it evolve through Glauber dynamics (inverse temperature β, zero magnetic field) for about ten Monte Carlo steps. In general, the resulting configuration will have a nonzero magnetization and we need to let it relax further till we have found some particular time where the magnetization goes through zero. Since we have set $\beta < 0$, the steady state is antiferromagnetic and initially $S(x, 0)$ has a sharp maximum (equal to 1) at $x = 0$, becomes negative for $x = 1$, and shows oscillations between positive and negative values for moderate x. For large x, it decays to zero. The remnants of this oscillatory behavior are still seen up to $t = 2$. For $t \geqslant 4$, $S(x, t)$ is nearly Gaussian, centered at some positive value $x_0(t)$. We focused on the moments of $S(x, t)$,

$$\langle 1 \rangle_t = \sum_{x=0}^{L} S(x, t) \tag{18a}$$

$$\langle x \rangle_t = \sum_{x=0}^{L} xS(x, t) \tag{18b}$$

$$\langle (x - \langle x \rangle_t)^2 \rangle_t = \sum_{x=0}^{L} (x - \langle x \rangle_t)^2 S(x, t) \tag{18c}$$

In practice, because the sampling of $S(x, t)$ is rather noisy for large x, the summations in Eqs. (18) are restricted to $x_- < x < x_+$, where x_+ is the first zero to the right and x_- the first zero to the left of the central peak of $S(x, t)$. Figure 3 shows $\langle x \rangle_t$, $\langle (x - \langle x \rangle_t)^2 \rangle_t$ versus t up to $t = 128$

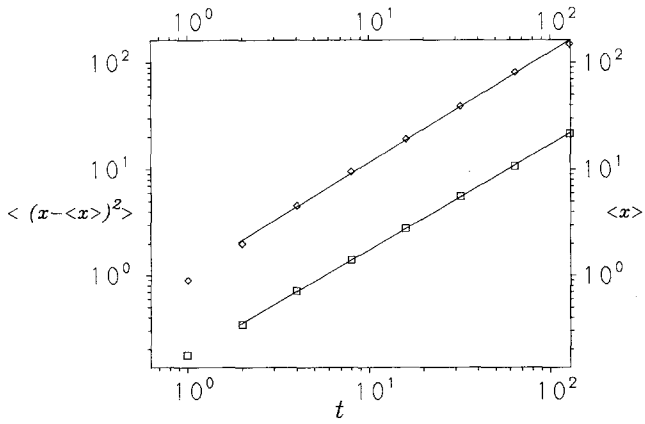

Fig. 3. Log-log plot of the moments of the structure function $S(x, t)$ versus time t, for $\alpha_1 = \alpha_2 = \frac{1}{2}$, $\alpha_3 = \alpha_4 = \frac{1}{4}$. (□) First moment $\langle x \rangle$ and (◇) second moment $\langle (x - \langle x \rangle_t)^2 \rangle_t$. System sizes are $L = 8192$ and averages have been taken over 100 samples.

for $\alpha_1 = \alpha_2 = 1/2$, $\alpha_3 = \alpha_4 = 1/4$. System sizes are $L = 8192$ and averages have been taken over 100 samples. We observed that $\langle 1 \rangle_t$ remained approximately constant, while $\langle x \rangle_t$ is proportional to t for $t > 4$. The truncated second moment scales as

$$\langle (x - \langle x \rangle_t)^2 \rangle_t \sim t^{2/z} \tag{19}$$

A least square fit to a straight line in the interval $4 \leqslant t \leqslant 128$ gives $z = 1.93 \pm 0.1$ and provides an independent check of the dynamic scaling exponent.

We also studied the dynamic structure function $S(k, t)$ in Fourier space. Simulations were done independently from those for $S(x, t)$, since $S(k, t)$ fluctuates considerably and must be averaged over a large number of samples. Linear fluctuation theory predicts that, in the hydrodynamic regime, k small, t large, with $k^2 t$ of order one, $S(k, t)$ should behave as

$$S(k, t) \simeq S(k, 0) \exp(-ict - Dk^2 t) \tag{20}$$

where $c = j'(0)$ is the sound velocity and D is the bulk diffusion coefficient. We simulated 10,240 systems of size $L = 512$, with $\alpha_1 = \alpha_2 = 1/2$ and $\alpha_3 = \alpha_4 = 1/4$. To remain in the hydrodynamic regime, only values for $k < 0.16 k_{\max}$ were retained ($k_{\max}$ is the edge of the first Brillouin zone). In this region, $S(k, 0)$ was approximately constant. To check (20), in Fig. 4, we plot $\log(|S(k, t)|/S(k, 0))$ versus $k^2 t$ for different times from $t = 1$ to $t = 128$. The data collapse well onto a single straight line, supporting the Gaussian character of $S(k, t)$.

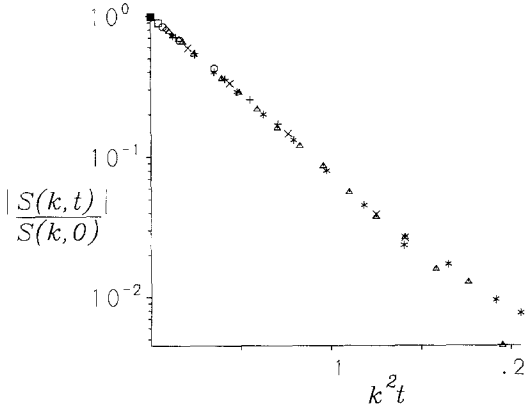

Fig. 4. Data collapse plot of $\log|S(k, t)|/S(k, 0)$ versus $k^2 t$ for different values of t: $t = 1$ (□), 2 (◇), 4 (△), 8 (○), 16 (+), 32 (×), 64 (∗), and 128 (△), with $\alpha_1 = \alpha_2 = = \frac{1}{2}$ and $\alpha_3 = \alpha_4 = \frac{1}{4}$. The system sizes are $L = 8192$ and averages have been over 10,240 samples, and over 10 different times for each sample.

4. CONCLUSIONS

Both the nonstationary width $w(t)$ and the stationary structure function yield the dynamical exponent $z=2$ within error bars. Furthermore, the structure function is approximately Gaussian. Thus, by conventional standards, our numerical results demonstrate convincingly that the cubic nonlinearity is marginally irrelevant.

On a theoretical level it can therefore be treated perturbatively. We investigate only the stationary fluctuations and follow the mode coupling analysis of van Beijeren *et al.*[6] (The methods of mode coupling theory are further explained in ref. 7). This leads to a nonlinear equation for the steady-state structure function $S(k, t)$ of the interface slope in a frame of reference moving with velocity c,

$$\frac{\partial}{\partial t} S(k, t) = -\nu k^2 S(k, t) - 6\lambda^2 k^2 S(k, 0)^{-1} \int_0^t ds\, S(k, t-s) S * S * S(k, s) \tag{21}$$

Here $S(k, 0)$ is the static structure function and the asterisk denotes convolution in k-space. The prefactor originates in a Gaussian factorization of the six-point function. We search for a scaling solution of the form $\exp\{-k^2[\nu t + at(\log(t)^\beta]\}$. Inserting this ansatz in Eq. (21) and taking the limit $k \to 0$ results in $\beta = 1/2$, $a = (12\pi/\sqrt{3})^{1/2}\lambda\chi$, with $\chi = S(k, 0)$ at $k=0$. Thus the truncated second moment of the structure function [see Eq. (18)] should grow in time as

$$\langle (x - \langle x \rangle_t)^2 \rangle_t \sim t(\log t)^{1/2} \tag{22}$$

We did not attempt to extract logarithmic corrections from our numerical data. However, the dynamic exponent z seems to lie systematically somewhat below two, which is consistent with the prediction (22).

ACKNOWLEDGMENTS

H.S. thanks B. Derrida, T. Hwa, D. Huse, J. L. Lebowitz, G. Speer, and H. van Beijeren for helpful discussions. This research is supported by the Deutsche Forschungsgemeinschaft. We are grateful to the HLRZ Jülich and the LRZ München for generous allocations of computer time.

REFERENCES

1. B. Derrida, J. L. Lebowitz, E. R. Speer, and H. Spohn, *Phys. Rev. Lett.* **67**:165 (1991).
2. M. Kardar, G. Parisi, and Y. C. Zhang, *Phys. Rev. Lett.* **56**:889 (1986).

3. J. Kertèsz and D. E. Wolf, *J. Phys. A* **21**:747 (1988).
4. J. Krug and H. Spohn, in *Solids Far from Equilibrium, Growth, Morphology and Defects*, C. Godrèche, ed. (Cambridge University Press, 1991).
5. B. M. Forrest and L. H. Tang, *Phys. Rev. Let.* **64**:1405 (1990).
6. H. van Beijeren, R. Kutner, and H. Spohn, *Phys. Rev. Lett.* **54**:2026 (1985).
7. T. Keyes, in *Modern Theoretical Chemistry, Statistical Physics II*, B. Berne, ed. (Plenum, New York, 1977).